Available online at www.sciencedirect.com

ScienceDirect

J Materiomics 1 (2015) 340−347

www.ceramsoc.com/en/

www.journals.elsevier.com/journal-of-materiomics/

Photocatalytic activity enhancement of modified g-C_3N_4 by ionothermal copolymerization

Han Zou [a], Xuehua Yan [a,b,*], Jie Ren [a], Xiao Wu [a], Yu Dai [a], Dawei Sha [a], Jianmei Pan [a], Jun Liu [c]

[a] School of Materials Science and Engineering, Jiangsu University, Zhenjiang 212013, Jiangsu, China
[b] Institute for Advanced Materials, Jiangsu University, Zhenjiang 212013, Jiangsu, China
[c] School of Environment and Safety Engineering, Jiangsu University, Zhenjiang 212013, Jiangsu, China

Received 4 May 2015; revised 24 October 2015; accepted 27 October 2015
Available online 5 November 2015

Abstract

The chemical structure and morphology of g-C_3N_4 were controlled. Dicyandiamide and barbituric acid were used as a co-precursor to graft aromatic groups in the tri-s-triazine structure unit and form the delocalized π-conjugate system. Meanwhile, lithium chloride and potassium chloride were used as heating media to restrain the agglomeration and keep the layered structure of the products. The results show that the as-prepared photocatalysts have a $(C_3N_4)_x$−$(C_7N_7)_y$ structure. According to the images by scanning electron microscopy (SEM) and transimisson electron microscopy (TEM) a clearly lamellar structure of the photocatalysts appears when the amount of barbituric acid is <0.86 g. The specific surface area can be increased by the ionothermal copolymerization synthesis method. Compared to g-C_3N_4-550, BA-CN_4 has a greater photocatalytic ability. The as-prepared photocalyst has a good degradation ratio after 4-run degradation of RhB dye recycle experiment.
© 2015 The Chinese Ceramic Society. Production and hosting by Elsevier B.V. This is an open access article under the CC BY-NC-ND license (http://creativecommons.org/licenses/by-nc-nd/4.0/).

Keywords: Carbon nitride; Copolymerization; Ionothermal; Photocatalysis

1. Introduction

Two-dimensional (2D) materials have attracted more attentions recently. As a graphite-like layered material, carbon nitride (C_3N_4) is used as a promising candidate for hydrogen evolution and environment purification under visible irradiation [1−4]. C_3N_4 has a broad application prospect for photocatalysis due to its unique semiconductor band structure, excellent chemical stability, high temperature stability and cheap raw materials [5−7]. However, some disadvantages like a high recombination rate of its photo-generated electron−hole pairs, low absorption intensity of visible light ($\lambda > 450$ nm) and aggregated structure restrict the application of C_3N_4 [8−10]. In order to overcome these disadvantages, C_3N_4 was modified with metallic elements (Fe, Ag, Co, Mn) [11−14], doped with non-metallic elements (B, S, P, F) [2,15−17] or composited with semiconductor (TiO_2, ZnO, CdS, Bi_2WO_6) [18−21] to improve the photocatalytic performance. Meanwhile, in some work [22−24], hard and soft templates were used to prepare nano-, meso- and micro-pore g-C_3N_4 and increase the specific surface area.

Zhang et al. [25] selected barbituric acid and dicyandiamide as a co-precursor to prepare the modified C_3N_4 polymer self-doped with carbon, resulting in a mixed C_3N_4−C_7N_7 structure. It was indicated that there is an enormous promotion of visible-light absorption region (up to 750 nm), which is realized by substituting the ring nitrogen with carbon, forming an extended delocalization π-conjugated system and changing the intrinsic semiconductor properties. Also, the more barbituric acid, the less the hydrogen evolution would be. This was

* Corresponding author. School of Materials Science and Engineering, Jiangsu University, Xuefu Road 301, Zhenjiang 212013, Jiangsu, China. Tel.: +86 511 88783268.
E-mail address: xhyan@mail.ujs.edu.cn (X. Yan).
Peer review under responsibility of The Chinese Ceramic Society.

http://dx.doi.org/10.1016/j.jmat.2015.10.004
2352-8478/© 2015 The Chinese Ceramic Society. Production and hosting by Elsevier B.V. This is an open access article under the CC BY-NC-ND license (http://creativecommons.org/licenses/by-nc-nd/4.0/).

since the excessive doping could spoil the indirect character of the semiconductor and offer some potential recombination sites.

Considering the special delocalization π-conjugated system and excellent visible-light absorption activity, we believe that it could be an outstanding photocatalyst to degrade organic pollutants. A preliminary work showed that the bulk g-C_3N_4 prepared by only dicyandiamide had a better photocatalytic activity than those photocatalysts prepared by copolymerization of dicyandiamide and barbituric acid. The degradation rate of those photocatalysts prepared by copolymerization was decreased when the mass of barbituric acid was increased, which was similar to the hydrogen evolution study above. It is suggested that the recombination of electron–hole pair could be accelerated due to the formation of agglomeration in the copolymerization process. As a consequence, it could be possible to improve the photocatalytic activity of g-C_3N_4 by designing a delocalization π-conjugated system and inhibiting the agglomeration of products simultaneously.

A crystalline, condensed and 2D carbon nitride was synthesized by an ionothermal method, which simply heated monomer with lithium chloride/bromide and potassium chloride/bromide [26–28]. Lithium chloride and potassium chloride are used as solvents due to their high-temperature stability, non-corrosive properties and melting point below the polycondensation point of s-heptazine. Noted that the condensation network could be facilitated by the solvation of the small molecular precursors and subsequent aggregation of higher molecular mass [27]. Therefore, a co-monomer was calcined by an ionothermal method to obtain the high visible-light absorption intensity and less agglomeration of carbon-nitrogen network for the enhancement of photocatalytic activity.

2. Experimental

2.1. Synthesis of photocatalysts

All the chemicals were used without further purification. The samples were synthesized *via* thermal treatment of completely mixed powders composed of 2 g dicyandiamide, 4.5 g lithium chloride (LiCl), 5.5 g potassium chloride (KCl) and different amounts of barbituric acid (0, 0.15, 0.27, 0.37, 0.52 and 0.86 g) in a tube furnace under N_2 atmosphere. The mixed powders were heated to 400 °C for 6 h, and then heated to 570 °C for 12 h with a heating rate of 7 °C/min. The resultant products were ground and then washed with distilled water for 3 times to remove residual salt, then ultrasonicated for 1 h and centrifuged at 10,000 rpm for 5 min before drying at 80 °C. The final products were obtained and denoted as BA-CN_0, BA-CN_1, BA-CN_2, BA-CN_3, BA-CN_4 and BA-CN_5, respectively (see Table 1). The bulk g-C_3N_4 was prepared by the same procedure above without LiCl and KCl, denoted as g-C_3N_4-570. Meanwhile, to compare to the photocatalytic ability of bulk g-C_3N_4 prepared at a lower temperature, 2 g dicyandiamide was heated to 400 °C for 6 h, and then heated to 550 °C for 12 h with a heating rate of 7 °C/min under the N_2 atmosphere. The product was denoted as g-C_3N_4-550.

Table 1
Reaction conditions for the preparation of photocatalysts.

	Dicyandiamide/g	LiCl/g	KCl/g	Barbituric acid/g	Temperature/°C
g-C_3N_4-550	2	–	–	–	550
g-C_3N_4-570	2	–	–	–	570
BA-CN_0	2	4.5	5.5	–	570
BA-CN_1	2	4.5	5.5	0.15	570
BA-CN_2	2	4.5	5.5	0.27	570
BA-CN_3	2	4.5	5.5	0.37	570
BA-CN_4	2	4.5	5.5	0.52	570
BA-CN_5	2	4.5	5.5	0.86	570

2.2. Characterization

The samples were characterized on a model Rigaku D/max2500 X-ray diffractometer for monochromatized Cu Kα (λ = 1.5406 Å) radiation. The XRD data were collected with a scanning speed of 5°/min in the 2θ range from 10° to 80°. The transmission electron microscopy (TEM) images were obtained by a model JEM-2100 (JEOL) transmission electron microscope. The microcrystalline structure and surface characteristics of the photocatalysts were observed by a model JSM-7001F field-emission scanning electron microscope (FE-SEM). The Fourier transformed infrared (FTIR) spectra were obtained using a model MX-1E (Nicolet) spectrometer at 600–4000 cm^{-1}. The diffuse reflection spectra (DRS) were obtained on a model Shimadzu UV-2450 spectrophotometer using $BaSO_4$ as a reference. The specific surface areas and pore structures were probed *via* the measurement of volumetric N_2 adsorption–desorption isotherms at liquid nitrogen temperature, using a NOVA 2000e instrument (Quantachrome, USA). The samples were degassed under vacuum at 120 °C for 8 h before measurements. The elemental analysis was performed on a model EA-1112 to obtain the mass ratio of carbon, nitrogen and hydrogen elements. The lithium quantification was performed by inductively coupled plasma mass spectrometry (ICP-MS) on an XSeries spectrometer.

2.3. Photocatalytic activity

The photocatalytic activities of the photocatalysts were determined in the degradation reaction of RhB aqueous solution (5 mg/L) under irradiation of a 125 W xenon light lamp with a 420 nm cutoff filter providing visible light irradiation. 100 mg of catalyst powder was added into 100 mL of the RhB solution in a quartz tube. Prior to irradiation, the suspension was magnetically stirred in dark for 50 min to establish an adsorption–desorption equilibrium between RhB and the catalyst. At the irradiation time intervals of 10 min, 5 mL suspension was collected and centrifuged to remove the particles. The RhB concentration was monitored at 553 nm during the photodegradation process using a UV–vis spectrophotometer.

3. Results and discussion

Fig. 1 shows the XRD patterns of g-C_3N_4-570 and BA-CN_x. Two peaks appear at 12.8° and 27.3° of the pure g-C_3N_4, which can be indexed to the (100) and (002) diffraction planes, due to the inter-planer packing and the characteristic inter-layer structural stacking peaks of the aromatic systems [5], respectively. The BA-CN_x sample has two main peaks at 12.8° and 27.3°, showing the formation of C_3N_4. The differences of diffraction angle and intensity between g-C_3N_4-570 and other samples indicate that the co-effects related to the molten salts and the quantity of barbituric acid can be described as follows: the diffraction angle is mainly affected by molten salts when the amount of barbituric acid is very small, but it will be mainly affected by barbituric acid at a certain amount. For instance, the molten salts lead to a smaller diffraction angle than 12.8° when the amount of barbituric acid is less than 0.15 g (i.e., BA-CN_0 and BA-CN_1). When the amount of baribituric acid is more than 0.27 g, it is interesting that the weight of barbituric acid has some effects on the two main peaks. The diffraction angle of 27.3° decreases, but the diffraction angle of 12.8° increases with increasing the amount of barbituric acid. This can be explained by the distortion of the tri-s-triazine unit due to the barbituric acid aromatic ring grafted in it, which occurred in plane instead of inter plane. The decreased quantity of hydrogen band, demonstrated by the FTIR spectra (see Fig. 4), leads to weaken the secondary bond and increases the distance between layers, which favors the exfoliation, proved by the decreased diffraction angles with increasing the amount of barbituric acid.

Fig. 2 shows the SEM images of the as-prepared samples of g-C_3N_4-570, BA-CN_0, BA-CN_3, and BA-CN_5, respectively. In Fig. 2(a), the sample g-C_3N_4-570 shows an obvious 2D lamellar structure with wrinkles. Compared to this disordered graphite-like flakes of g-C_3N_4-570, BA-CN_0 (see Fig. 2(b)) and BA-CN_3 (see Fig. 2(c)) are more likely ordered sheets, which can be explained by the physical effects of molten salt during the heating procedure. In Fig. 2(d), BA-CN_5 has disordered sheets, which are probably induced by the excessive barbituric acid.

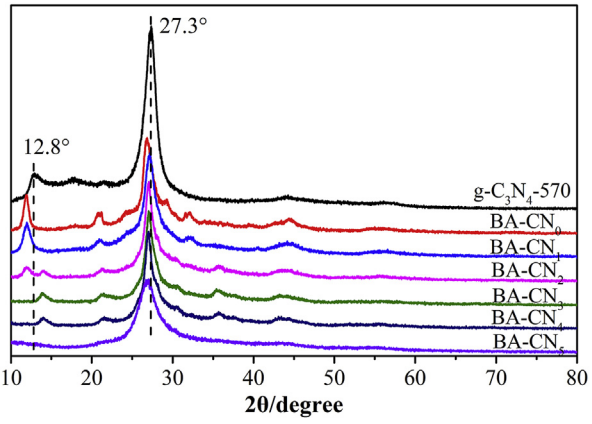

Fig. 1. XRD patterns of the as-prepared samples: g-C_3N_4-570, BA-CN_0, BA-CN_1, BA-CN_2, BA-CN_3, BA-CN_4 and BA-CN_5.

Fig. 3 shows the TEM images of the as-synthesized g-C_3N_4-570, BA-CN_0, BA-CN_3 and BA-CN_5, respectively. In Fig. 3(a), the morphology of g-C_3N_4 is bulk with a lamellar structure at the edges [29]. In Fig. 3(b), BA-CN_0 clearly shows large sheets composed of some irregular but micro-fragments with the sizes of 10–50 nm. According to Bojdys et al. [27], the hexagonal prisms were not generated because the samples were not prepared at a high temperature (i.e., 600 °C) and airtight condition. BA-CN_3 is composed of some micro-fragments, which is similar to BA-CN_0, except for the obviously agglomerated products induced by the addition of barbituric acid. In Fig. 3(d), the overweight of barbituric acid can decrease the features of platelike and microcrystalline [25].

Fig. 4 shows the FT-IR spectra of the as-prepared photocatalysts in the wavelength range of 500–3500 cm^{-1}. The band at 810 cm^{-1} is a characteristic of tri-s-triazine. The bands located in the range of 1242–1637 cm^{-1} are contributed to the typical stretching modes of CN heterocyles, which shift slightly due to the addition of the barbituric acid and LiCl/KCl. The board peak at 3163 cm^{-1} of bulk g-C_3N_4 corresponding to the N–H band involving with hydrogen bond in- and inter-plane moves to 3380 cm^{-1} (see Fig. 4), indicating the presence of $-NH_2$ and –NH but the absence of hydrogen bond in the polymer network prepared by ionothermal copolymerization [30]. In addition, the band at 2163 cm^{-1} is attributed to the C≡N band stretching vibration modes [31], which can be found in the samples except g-C_3N_4-570. The reason for this is probably because of the deformation of CN heterocyles induced by the high temperature treatment and the existence of LiCl/KCl.

Fig. 5 shows the UV–vis absorption spectra for the as-prepared samples. Clearly, there is an obvious red shift and the light absorption intensity in the range of visible light wavelength increases when barbituric acid content increases, compared to that from g-C_3N_4-570 [25]. The red shift of the absorption wavelength favors the photocatalysts to generate more electron–hole pairs under sunlight irradiation, resulting in enhanced photocatalytic properties. Fig. 5 also shows an unobvious regular pattern of light absorption, which may be due to the complicated chemical structure developed in the copolymerization with molten salts. It is speculated that the molten salts inhibit the diffusion of babituric acid molecules. As a consequence, C_3N_4 and C_7N_7 units are unregularly distributed in the network, leading to the differences of delocalized π-conjugate system among these samples. BA-CN_0 shows a blue shift of the optical absorption, which could be ascribed to the changed electronic structure induced by the Li^+ or other ions. The existence of Li element is determined by ICP-MS.

The elemental analysis was further used to determine the mole ratio of carbon to nitrogen (C:N) in the products. The C:N value of g-C_3N_4-570, BA-CN_0, BA-CN_1, BA-CN_2, BA-CN_3, BA-CN_4 and BA-CN_5 is 0.658, 0.679, 0.766, 0.783, 0.809, 0.844 and 0.908, respectively. It means that the aromatic ring is indeed grafted in tri-s-triazine unit and the C_7N_7 structure is formed, resulting in an increased content of carbon element and the formation of delocalized π-conjugate system,

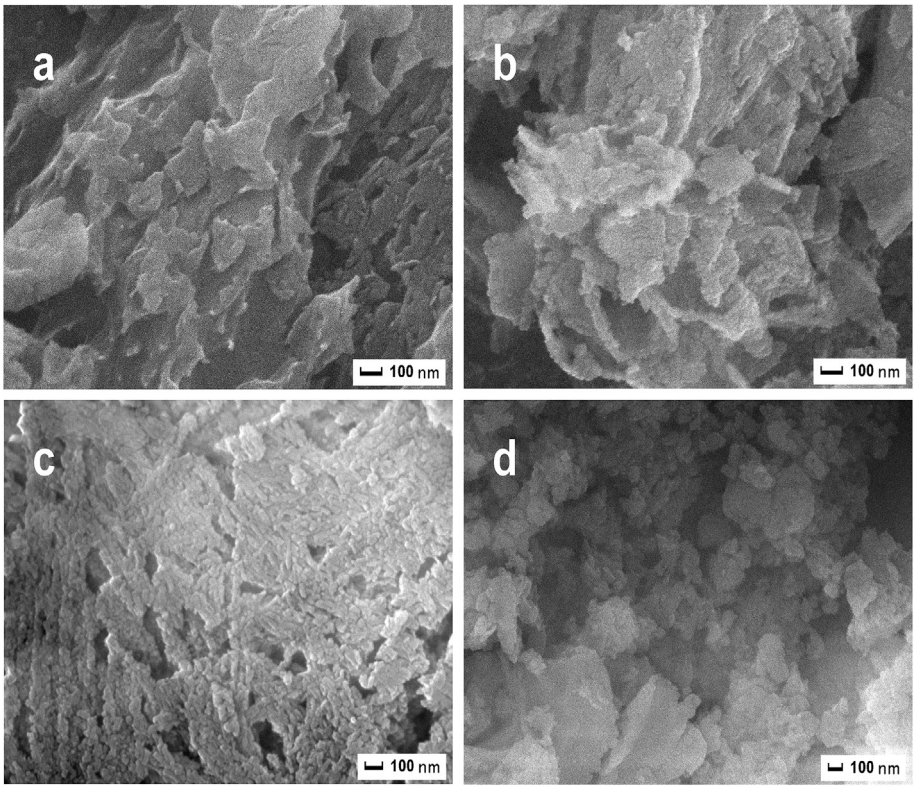

Fig. 2. SEM images of the as-prepared samples: (a) g-C_3N_4-570, (b) BA-CN_0, (c) BA-CN_3, (d) BA-CN_5.

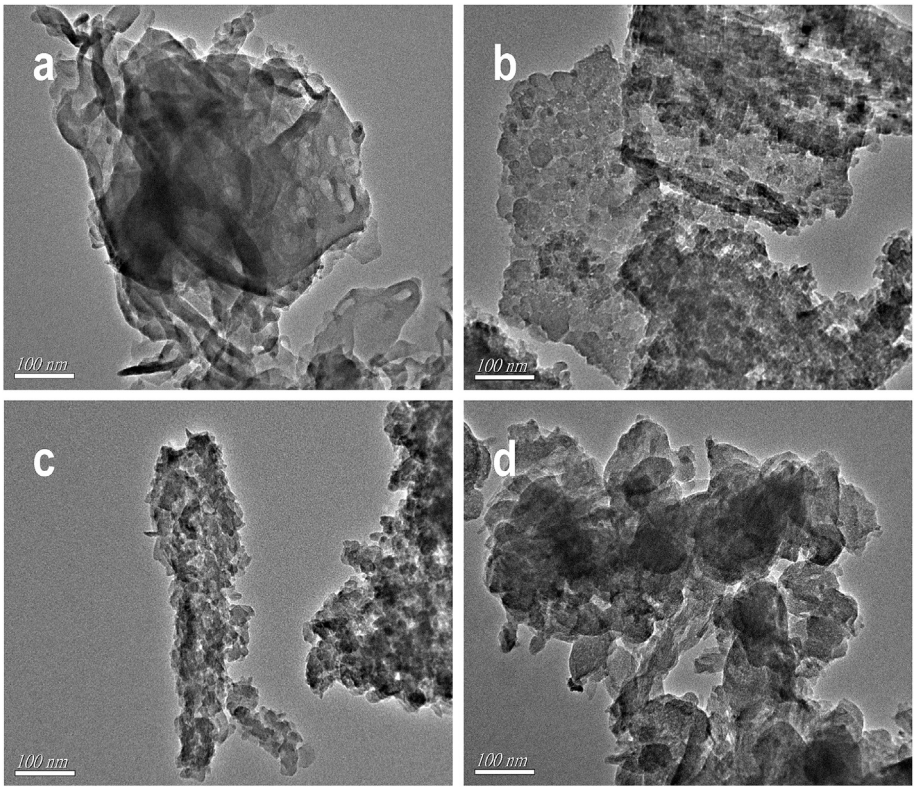

Fig. 3. TEM images of the as-prepared samples: (a) g-C_3N_4-570, (b) BA-CN_0, (c) BA-CN_3, (d) BA-CN_5.

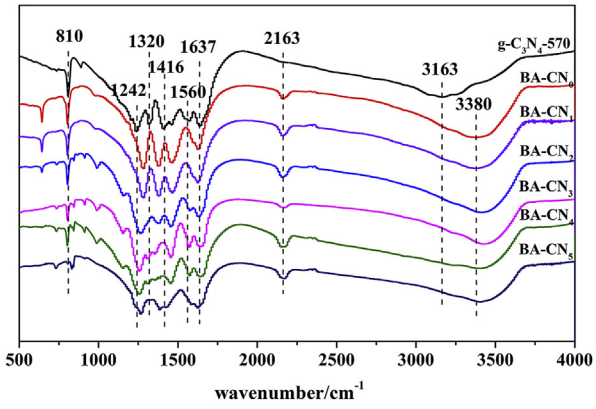

Fig. 4. FT-IR spectra of g-C_3N_4-570, BA-CN_0, BA-CN_1, BA-CN_2, BA-CN_3, BA-CN_4 and BA-CN_5.

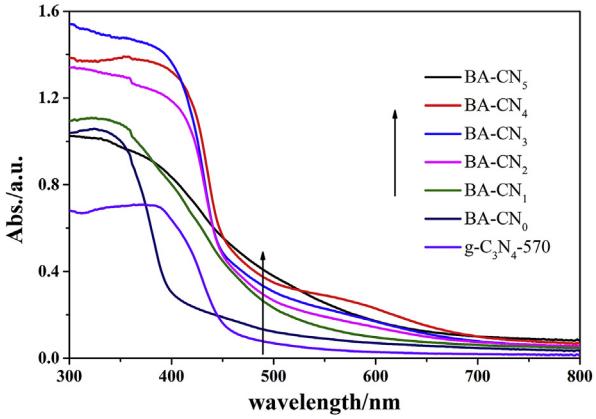

Fig. 5. UV–vis absorption spectra for the as-prepared samples.

which can change the intrinsic semiconductor properties. It is assumed that the basic structural unit of BA-CN_3 should be $(C_3N_4)_x$–$(C_7N_7)_y$. When the mole ratio of C:N is 0.809, the value of x:y is 5.67. Table 2 shows the calculated results of others. We attributed the deviation of C:N with stoichiometry of C_3N_4 to the structure defects, such as the –NH, $-NH_2$ and –C≡N groups.

Fig. 6 shows the N_2 sorption isotherms and pore size distribution curves (BJH) of BA-CN_0, BA-CN_1, BA-CN_2, BA-CN_3, BA-CN_4, BA-CN_5, and g-C_3N_4-570, respectively. The corresponding pore size distribution curves are determined from the desorption branches using Barret-Joyner-Halender method (see the inset in Fig. 6). In Table 2, the specific surface area of BA-CN_x increases greatly by ionothermal copolymerization synthesis method. The sample BA-CN_3 has the greatest specific surface area, explaining the clearly adsorption of RhB in the dark (see Fig. 7). The excessive doping of barbituric acid decreases the specific surface area.

Fig. 7 shows (a) the photocatalytic degradation of RhB as a function of irradiation time for g-C_3N_4-570, BA-CN_0, BA-CN_1, BA-CN_2, BA-CN_3, BA-CN_4 and BA-CN_5 samples under visible light irradiation, (b) the photocatalytic activity of g-C_3N_4-550, g-C_3N_4-570 and BA-CN_4, and (c) the relationship between the RhB degradation efficiency and the light irradiation time, respectively. In Fig. 7(a), the photocatalytic activity of photocatalysts increases by increasing the content of barbituric acid to 0.86 g, due to that the excessive doping spoils the indirect character of the semiconductor and offers potential recombination sites [25]. The sample BA-CN_3 exhibits a more intense adsorption to RhB dye rather than the other samples, which is improved using an appropriate amount of barbituric acid.

The photocatalytic ability of g-C_3N_4 is related with the synthesis temperature [2]. It is necessary to distinguish the contribution of two factors, which are the synthesis temperature and ionothermal copolymerization process. In Fig. 7(b), a higher synthesis temperature for g-C_3N_4-550 leads to a better photocatalytic ability, compared to g-C_3N_4-570 [2]. Also, the ionothermal copolymerization can improve the photocatalytic ability of BA-CN_4, compared to g-C_3N_4-570. The ratio of degrading RhB increases from 41.5% (g-C_3N_4-550) to 83.8% (BA-CN_4) after irradiating under visible light for 90 min, which is calculated according to the formula as $\eta = (C_1 - C)/C_1$ (where C_1 and C are the relative concentrations of RhB at 0 and 90 min, respectively), indicating the increase of the photocatalytic activity by ionothermally copolymerized at a high temperature.

The kinetics of RhB photodecomposition on the catalyst surface can be described by the first-order equation

$$\ln\left(\frac{C_0}{C}\right) = kt \quad (1)$$

where k is the rate constant (min^{-1}), C_0 is the initial concentration of target dye, and C is the actual concentration of target dye at light irradiation time t. In Fig. 7(c), the k value increases gradually with increasing the amount of barbituric acid until 0.86 g, which is because the excessive doping of aromatic groups spoils the indirect character of the semiconductor and offers potential recombination sites. The sample BA-CN_4 shows the maximal k value of 0.02031 min^{-1} because it has the best $(C_3N_4)_x$–$(C_7N_7)_y$ equilibrium and no severe agglomeration. The sample BA-CN_0 shows the lowest degradation ratio because the excessive ions existed in the polymer network changed its energy band structure, thus decreasing its visible light absorption activity (see Fig. 5).

Fig. 8 shows the recycled experimental results of the photodegradation of RhB catalyzed by BA-CN_4. Clearly, the photocatalytic activity of BA-CN_4 has no apparent deactivation (the degradation ratio is 80%) after 4 recycles for the degradation of RhB under visible light irradiation, revealing that the photocatalyst possesses a good stability. Moreover, Fig. 9 shows the XRD pattern of BA-CN_4 after 4-run recycles. The sample BA-CN_4 still has a good degradation ratio after 4-run recycles although the diffraction peaks decrease in the XRD pattern.

4. Conclusions

Carbon nitride contained $(C_3N_4)_x$–$(C_7N_7)_y$ unit was synthesized by heating dicyandiamide and barbituric acid as the

Table 2
Experimental C/N mole ratio, the value of x:y and surface area of samples.

	g-C_3N_4-570	BA-CN_0	BA-CN_1	BA-CN_2	BA-CN_3	BA-CN_4	BA-CN_5
Experimental C/N mole ratio	0.658	0.679	0.766	0.783	0.809	0.844	0.908
Value of x:y	–	–	25.59	11.51	5.67	2.90	1.01
Surface area (m^2/g)	20.848	137.585	149.089	171.463	246.066	175.380	164.209

co-precursor in lithium chloride and potassium chloride as media. Based on the analysis by X-ray diffraction, the structure characteristic of the as-prepared photocatalysts was similar to that of bulk g-C_3N_4. In the SEM and TEM images, an obvious layered structure of BA-CN_x occurred. In the FT-IR spectra, BA-CN_x had the similar groups as bulk g-C_3N_4. The UV–vis spectra indicated that BA-CN_x had an obvious red shift and an increased light absorption intensity, compared to bulk g-C_3N_4. The specific surface area of BA-CN_x could be increased by the ionothermal copolymerization synthesis method. The photocatalytic degradation of RhB under visible light showed the optimum photocatalytic ability of BA-CN_4 when the weight of barbituric acid was 0.52 g, because it had the best $(C_3N_4)_x$–$(C_7N_7)_y$ equilibrium and no severe

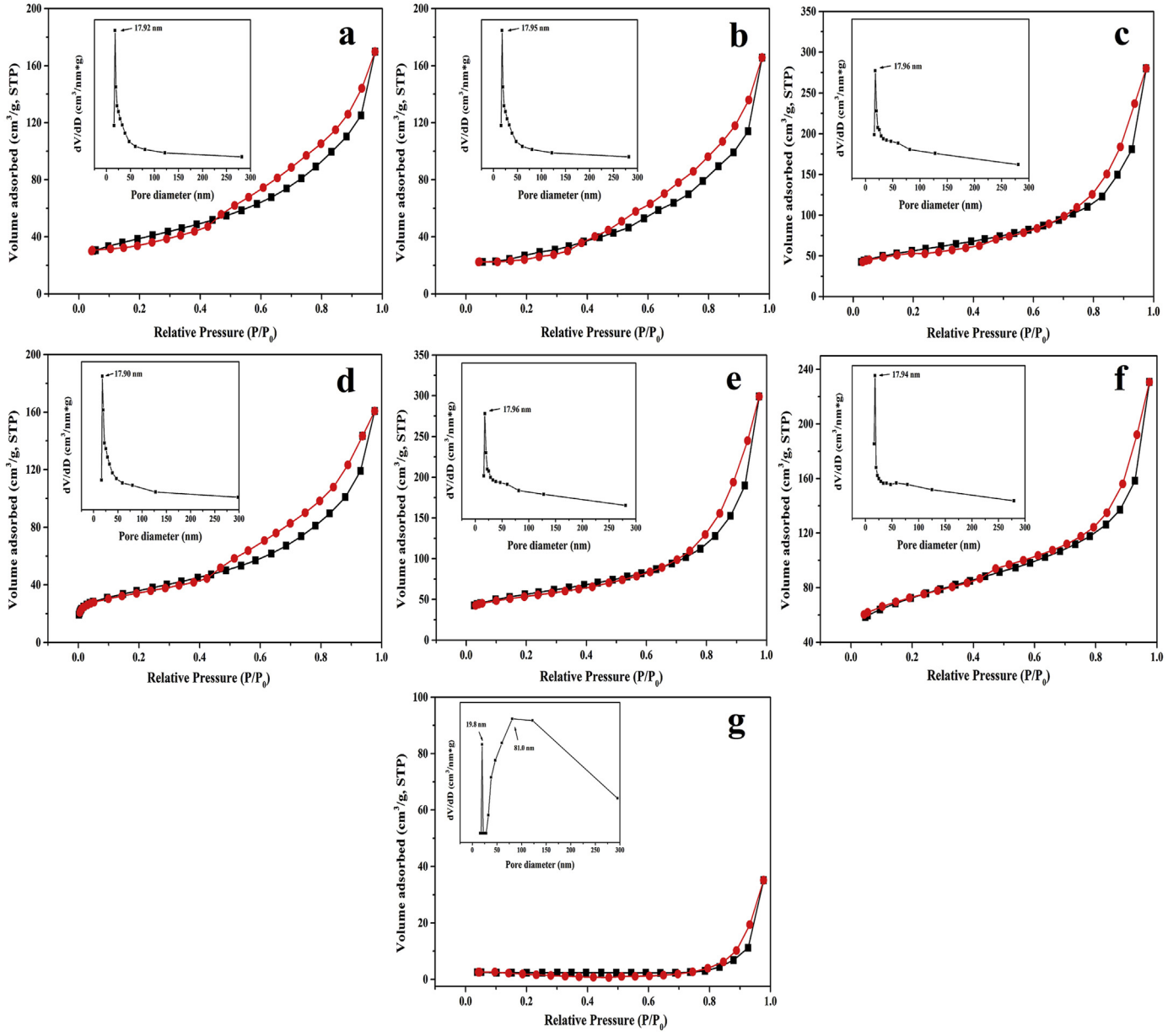

Fig. 6. N_2 sorption isotherms and pore size distribution curves (BJH): (a) BA-CN_0, (b) BA-CN_1, (c) BA-CN_2, (d) BA-CN_3, (e) BA-CN_4, (f) BA-CN_5, (g) g-C_3N_4-570.

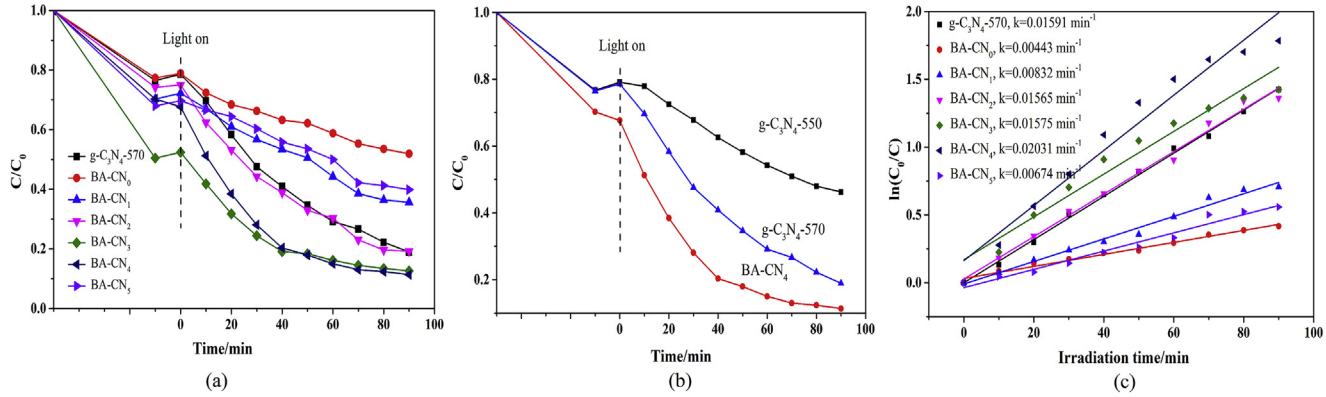

Fig. 7. (a) Photocatalytic degradation of RhB as a function of irradiation time over g-C_3N_4-570, BA-CN_0, BA-CN_1, BA-CN_2, BA-CN_3, BA-CN_4 and BA-CN_5 samples under visible light irradiation. (b) The photocatalytic activity of g-C_3N_4-550, g-C_3N_4-570 and BA-CN_4. (c) Relationship between the RhB degradation efficiency and the light irradiation time.

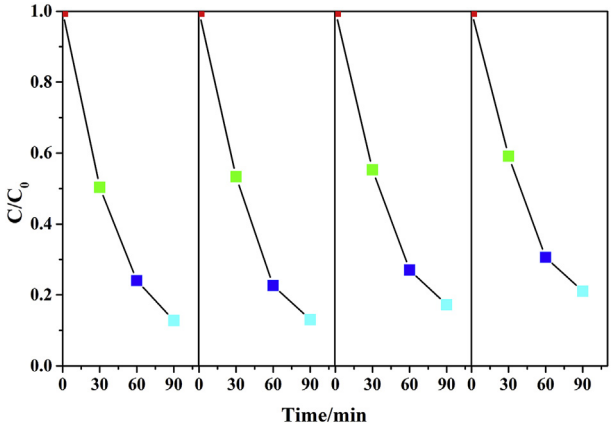

Fig. 8. Recycled experimental results of the photodegradation of RhB catalyzed by BA-CN_4.

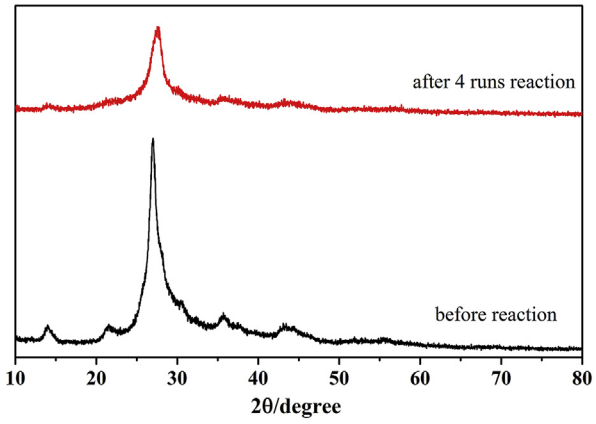

Fig. 9. XRD patterns of BA-CN_4 before and after 4-run recycles.

agglomeration. The photocatalytic property was also stable after 4-run recycles.

Acknowledgments

This work was financially supported by National Natural Science Foundation of China (51502116), the Six Talents Peak Project in Jiangsu Province (2011-ZBZZ045), the Jiangsu Province Research Joint Innovation Fund-Prospective Joint Research Project (BY2014123-08), the Jiangsu Province Ordinary University Graduate Student Innovation Project (SJLX_0462, SJLX15_0489).

References

[1] Schwinghammer K, Mesch MB, Duppel V, Ziegler C, Senker J, Lotsch BV. Crystalline carbon nitride nanosheets for improved visible-light hydrogen evolution. J Am Chem Soc 2014;136:1730–3.

[2] Yan SC, Li ZS, Zou ZG. Photodegradation of rhodamine B and methyl orange over boron-doped g-C_3N_4 under visible light irradiation. Langmuir 2010;26:3894–901.

[3] Obregon S, Colon G. Improved H_2 production of Pt-TiO_2/g-C_3N_4-MnO_x composites by an efficient handling of photogenerated charge pairs. Appl Catal B Environ 2014;144:775–82.

[4] Liu W, Wang ML, Xu CX, Chen SF. Facile synthesis of g-C_3N_4/ZnO composite with enhanced visible light photooxidation and photoreduction properties. Chem Eng J 2012;209:386–93.

[5] Jiang DL, Chen LL, Zhu JJ, Chen M, Shi WD, Xie JM. Novel p-n heterojunction photocatalyst constructed by porous graphite-like C_3N_4 and nanostructured BiOI: facile synthesis and enhanced photocatalytic activity. Dalton Trans 2013;42:15726–34.

[6] Wang XC, Maeda K, Thomas A, Takanabe K, Xin G, Carlsson JM, et al. A metal-free polymeric photocatalyst for hydrogen production from water under visible light. Nat Mater 2009;8:76–9.

[7] Yan SC, Li ZS, Zou ZG. Photodegradation performance of g-C_3N_4 fabricated by directly heating melamine. Langmuir 2009;25:10397–401.

[8] Xu L, Xia JX, Xu H, Yin S, Wang K, Huang LY, et al. Reactable ionic liquid assisted solvothermal synthesis of graphite-like C_3N_4 hybridized α-Fe_2O_3 hollow microspheres with enhanced supercapacitive performance. J Power Sources 2014;245:866–74.

[9] Tonda S, Kumar S, Kandula S, Shanker V. Fe-doped and-mediated graphitic carbon nitride nanosheets for enhanced photocatalytic performance under natural sunlight. J Mater Chem A 2014;2:6772–80.

[10] Zhou XS, Jin B, Chen RQ, Peng F, Fang YP. Syntheses of porous Fe_3O_4/g-C_3N_4 nanospheres as highly efficient and recyclable photocatalysts. Mater Res Bull 2013;48:1447–52.

[11] Wang XC, Chen XF, Thomas A, Fu XZ, Antonietti M. Metal-containing carbon nitride compounds: a new functional organic-metal hybrid material. Adv Mater 2009;21:1609–12.

[12] Zhou T, Xu YG, Xu H, Wang HF, Da ZL, Huang SQ, et al. In situ oxidation synthesis of visible-light-driven plasmonic photocatalyst Ag/AgCl/g-C_3N_4 and its activity. Ceram Int 2014;40:9293–301.

[13] Liu Q, Zhang JY. Graphene supported co-g-C_3N_4 as a novel metal−macrocyclic electrocatalyst for the oxygen reduction reaction in fuel cells. Langmuir 2013;29:3821−8.
[14] Ghosh D, Periyasamy G, Pandey B, Pati SK. Computational studies on magnetism and the optical properties of transition metal embedded graphitic carbon nitride sheets. J Mater Chem C 2014;2:7943−51.
[15] Liu G, Niu P, Sun CH, Smith SC, Chen ZG, (Max) Lu GQ, Cheng HM. Unique electronic structure induced high photoreactivity of sulfur-doped graphitic C_3N_4. J Am Chem Soc 2010;132:11642−8.
[16] Hu SZ, Ma L, You JG, Li FY, Fan ZP, Wang F, et al. A simple and efficient method to prepare a phosphorus modified g-C_3N_4 visible light photocatalyst. RSC Adv 2014;4:21657−63.
[17] Wang Y, Di Y, Antoietti M, Li HR, Chen XF, Wang XC. Excellent visible-light photocatalysis of fluorinated polymeric carbon nitride solids. Chem Mater 2010;22:5119−21.
[18] Yan HJ, Yang HX. TiO_2-g-C_3N_4 composite materials for photocatalytic H_2 evolution under visible light irradiation. J Alloys Compd 2011;509:L26−9.
[19] Sun JX, Yuan YP, Qiu LG, Jiang X, Xie AJ, Shen YH, et al. Fabrication of composite photocatalyst g-C_3N_4-ZnO and enhancement of photocatalytic activity under visible light. Dalton Trans 2012;41:6756−63.
[20] Ge L, Zou F, Liu JK, Ma Q, Wang C, Sun DZ, et al. Synthesis and efficient visible light photocatolytic hydrogen evolution of polymeric g-C_3N_4 coupled with CdS quantum dots. J Phys Chem C 2012;116:13708−14.
[21] Ge L, Han CC, Liu J. Novel visible light-induced g-C_3N_4/Bi_2WO_6 composite photocatalysts for efficient degradation of methyl orange. Appl Catal B Environ 2011;108:100−7.
[22] Wang XC, Maeda K, Chen XF, Takanabe K, Domen K, Hou YD, et al. Polymer semiconductors for artificial photosynthesis: hydrogen evolution by mesoporous graphitic carbon nitride with visible light. J Am Chem Soc 2009;131:1680−1.
[23] Yan HJ. Soft-templating synthesis of mesoporous graphitic carbon nitride with enhanced photocatalytic H_2 evolution under visible light. Chem Commun 2012;48:3430−2.
[24] Xu J, Wang YJ, Zhu YJ. Nanoporous graphitic carbon nitride with enhanced photocatalytic performance. Langmuir 2013;29:10566−72.
[25] Zhang JS, Chen XF, Takanabe K, Maeda K, Domen K, Epping JD, et al. Synthesis of a carbon nitride structure for visible-light catalysis by copolymerization. Angew Chem Int Ed 2010;49:441−4.
[26] Wirnhier E, Döblinger M, Gunzelmann D, Senker J, Lotsch BV, Schnick W. Poly(triazine imide) with intercalation of lithium and chloride ions $[(C_3N_3)_2(NH_xLi_{1-x})_3\cdot LiCl]$: a crystalline 2D carbon nitride network. Chem Eur J 2011;17:3213−21.
[27] Bojdys MJ, Müller JO, Antonietti M, Thomas A. Ionothermal synthesis of crystalline, condensed, graphitic carbon nitride. Chem Eur J 2008;14:8177−82.
[28] Chong SY, Jones JTA, Khimyak YZ, Cooper AI, Thomas A, Antonietti M, et al. Tuning of gallery heights in a crystalline 2D carbon nitride network. J Mater Chem A 2013;1:1102−7.
[29] Chai B, Peng TY, Mao J, Li K, Zan L. Graphitic carbon nitride (g-C_3N_4)-Pt-TiO_2 nanocomposite as an efficient photocatalyst for hydrogen production under visible light irradiation. Phys Chem Chem Phys 2012;14:16745−52.
[30] Jürgens B, Irran E, Senker J, Kroll P, Müller H, Schnick W. Melem (2,5,8-Triamino-tri-s-triazine), an important intermediate during condensation of melamine rings to graphitic carbon nitride: synthesis, structure determination by X-ray powder diffractometry, solid-state NMR, and theoretical studies. J Am Chem Soc 2003;125:10288−300.
[31] Schmidt CL, Jansen M. New directions in carbonitride research: synthesis of resin-like dense-packed C_3N_4 using a hydrogen-free precursor. J Mater Chem 2010;20:4183.

Prof. Dr. Xuehua Yan: a Professor in Institute for Advanced Materials, Jiangsu University, China. He got his Ph.D. in 2006 from Jiangsu University, worked in Technical University of Darmstadt (Germany) in 2008 as a visiting Professor and collaborated with Prof. Dr. Ralf Riedel. His research focuses on functional inorganic materials and composites, including photocatalytic nanomaterials, negative thermal expansion materials and porous materials. He has published 100 papers and 12 national patents. He is a member of the editorial committee of *Journal of the Chinese Ceramic Society.*